This article has been accepted for publication in a future issue of this journal, but has not been fully edited. Content may change prior to final publication. Citation information: DOI 10.1109/TAP.2017.2670328, IEEE Transactions on Antennas and Propagation

A Fast Estimation Technique for Evaluating the Specific Absorption Rate of Multiple-Antenna Transmitting Devices

Dinh Thanh Le, Lira Hamada, Soichi Watanabe, and Teruo Onishi, *Members, IEEE*

***Abstract*—In this paper, we present a fast technique for estimating the specific absorption rate (SAR) of multiple-antenna transmitting devices such as mobile phones, which utilize two or more antennas in communication. SAR values for arbitrary relative phase combinations of the antennas at an observation point can be estimated from SAR measurements for several known relative phases at the same observation point. Several numerical and experimental validations on different antenna configurations and operating frequencies have been carried out to verify the proposed estimation method. It has been highlighted that the proposed estimation method is simple yet provides highly accurate estimated SAR values.**

***Index Terms*—SAR, estimation, multiple-antenna transmitting, MIMO.**

I. Introduction

In recent years, multiple antennas working at the same frequency have been increasingly employed in many wireless communication devices with different techniques such as multi-input multi-output (MIMO) or phased antenna arrays. Therefore, there is an increasing demand to develop measurement methods and procedures for evaluating the specific absorption rate (SAR) of such devices in compliance tests for radio frequency radiation protection guidelines [1]. SAR indicates the amount of power absorbed per unit mass of a biological body when it is exposed to an electromagnetic field. In SAR measurements, the biological body is represented by a dielectric medium, which has dielectric constants similar to that of the biological body, and called a phantom. SAR is proportional to the power of the internal electric field ($|E|^2$) and is expressed as

$$\mathrm{SAR} = \frac{\sigma\,|E|^2}{\rho} \quad [W/kg], \tag{1}$$

where σ and ρ represent the electric conductivity (S/m) and mass density (kg/m^3) of the medium, respectively.

There are two types of electric field probe used to measure SAR: vector electric field probes and scalar electric field ones. The scalar electric field probes can provide only information of the magnitude of measured electric fields, whereas the vector electric field probes can give information of both the phase and magnitude of measured electric fields. However, while the scalar probes are widely used in laboratories and relatively inexpensive, the vector probes might be expensive and not readily available at present. SAR can be measured using electric field probes and calculated according to Eq. (1).

If only one transmitting antenna is considered, which is the typical case for conventional devices with one transmitting antenna for communication, SAR does not depend on the phase but on the magnitude of the measured electric field. Measurement procedures for such devices are defined in international standards [2], [3], and improved in fast SAR measurement techniques from 2-D area scans [4], or using vector electric field probes [5], [6]. However, when there are two or more transmitting antennas simultaneously working at the same frequency in the device under test (DUT), the total electric field is the vector summation of the electric fields from individual antennas. Thus, the total electric field at each measured point will strongly depend on the relative phases of the radiating sources. Therefore, the SAR of multiple-antenna transmitting devices will change according to the change in the relative phase of the radiating sources. This problem remains a challenging issue when one measures the SAR of multiple antenna transmitters such as MIMO or phased array antenna systems.

Some recent works on electromagnetic field compliance assessments of radio base stations utilizing antenna arrays provide analyses to evaluate electric fields radiated from multi-band and multi-antenna base stations, where field combining methods for uncorrelated and correlated exposure were applied [7], [8]. For multi-antenna hand-held devices, a technical report of the International Electrotechnical Commision (IEC) [9], and current SAR measurement standards [2], [3] recommend measuring SAR repetitively with every combination of the relative phases and magnitude of the sources. For instance, in the case of two transmitting antennas, measurement needs to be conducted with every relative phase combination of the sources, sweeping from 0 to 360 degree with a phase step. If the phase step is equal to 10 degree, for example, there would be 36 repetitive measurements in order to find the maximum SAR corresponding to a particular relative phase combination. Clearly, this technique is considerably time-consuming owing to the large number of the relative phase combination, particularly when many antennas are utilized in

D. T. Le, L. Hamada, and S. Watanabe are with the Electromagnetic Compatibility Laboratory, National Institute of Information and Communications Technology (NICT), Koganei, Tokyo 184-8795, Japan. E-mail: {ledt; hamada; wata}@nict.go.jp.

Currently, D. T. Le is with the Faculty of Radio-Electronics Eng., Le Quy Don Technical University (LQDTU), 236 Hoang Quoc Viet, Hanoi, Vietnam. Email: le.dinhthanh.vn@ieee.org.

T. Onishi are with NTT DOCOMO, Inc., 3-6 Hikarino-oka, Yokosuka, Kanagawa 239-8536, Japan. Email: oonishite@nttdocomo.co.jp.

Manuscript received November 6, 2015; revised May 12, 2016 and December 12, 2016; accepted December 28, 2016.

This article has been accepted for publication in a future issue of this journal, but has not been fully edited. Content may change prior to final publication. Citation information: DOI 10.1109/TAP.2017.2670328, IEEE Transactions on Antennas and Propagation

a device and/or the phase step is small.

To reduce the measurement time, some other measurement methods were introduced. Namely, antennas are turned ON or OFF alternatively during the SAR measurement. The SAR corresponding to the active (ON) antennas will be measured separately, and the total SAR value will then be determined by combining the individual measured SAR [10]. This method, however, can only provide an upper bound of the SAR, thus potentially overestimating the actual SAR. Nevertheless, it also requires additional switches to turn antennas ON or OFF, thus making the test modes of measurement devices more complicated.

In addition, another method, where all antennas are activated during the SAR measurement, was also proposed by our research group [6]. This method allows taking a time-averaged SAR value during a certain averaging period with a conventional SAR measurement system using scalar electric field probes. The advantages of this method are (i) the control of the relative phases of the antennas is not required, and (ii) it is applicable to devices where the phase and amplitude of the transmitting signals change during operations (amplitude and phase modulation) such as MIMO or multiple input single output (MISO) communications. However, the disadvantages of this method include (i) a longer averaging time (measurement time) compared with the conventional single-antenna transmitting devices, and (ii) potential underestimation for the devices where the phase and amplitude of transmitting signals do not change during a certain time of operations such as smart antenna or array antenna devices.

In this paper, we present a fast and highly accurate estimation method for evaluating the SAR values for arbitrary relative phase combinations. Only several measurements for pre-known relative phase combinations should be conducted. The SAR for any other relative phase combinations can be estimated on the basis of the measured data. The proposed estimation method can be well applied to conventional SAR measurement systems using a scalar electric field or to advanced SAR measurement systems using vector electric field probes. Generally, in a device consisting of N-element transmitting antennas, only N measurements for N known relative phases are necessary for measurement systems with vector electric field probes. On the other hand, $N(N-1)+1$ measurements are required for measurement systems utilizing scalar electric field probes. By reducing the number of measurements, the proposed estimation method provides a practical procedure for evaluating the SAR for multiple-antenna transmitting devices, and thus is promisingly applicable to compliance tests.

The rest of this paper is organized as follows. In section II, the fundamental concepts of the proposed estimation method and field analyses will be presented. A measurement procedure based on the proposed estimation method is also illustrated in this section. Numerical and experimental validations will be shown in sections III and IV with various types of antenna configurations, respectively. Discussions about the proposed method and related works will be presented in section V, followed by concluding remarks in section VI.

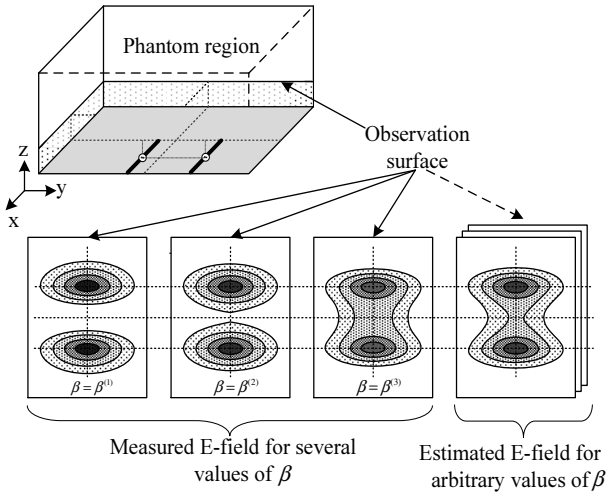

Fig. 1. Estimation concepts for a two-element antenna array.

II. Fundamental estimation concepts

A. Two-antenna case

Let us first consider the simplest case of a multiple-antenna transmitting devices which consists of two antennas simultaneously working at the same frequency. The total field at a measurement point inside a phantom depends on the phase and magnitude of the electric fields from the individual antennas. To make it simple, we assume that only relative phases of the sources are considered as subject to change whereas the time-averaged value of the magnitude is kept unchanged at their maximum values. This assumption is quite reasonable for evaluating the maximum local SAR because it normally corresponds to the maximum power of feeding sources.

Figure 1 shows estimation concepts for a simple configuration of a two-antenna array placed below a flat phantom. Note that this method can also be applicable to a non-flat phantom such as the SAM phantom. At a measurement point (P), the total electric field (including the three components x, y, z) is equal to the vector summation of the individual electric field from each antenna. It can be given as

$$E = E_1 + E_2 e^{j\beta} \tag{2}$$

where β is the relative phase of the two antennas, and E_1 and E_2 are the electric fields from antennas 1 and 2, respectively. This equation is true for the three components x, y, and z of the electric fields: thus, the following developments of equations can be applied for all components, and therefore the proposed estimation method will be independent of the field polarizations.

Now, to avoid duplication in notations, let $a_1 = E_1$ and $a_2 = E_2$ (complex values). Then, Eq. (2) can be re-written as

$$E = a_1 + a_2 e^{j\beta}. \tag{3}$$

Regarding the change in the relative phase of the antennas at the same evaluation point (P), it is important to note that the factors a_1 and a_2 do not depend on β. Thus, we can consider the total electric field in Eq. (3) as a function of

This article has been accepted for publication in a future issue of this journal, but has not been fully edited. Content may change prior to final publication. Citation information: DOI 10.1109/TAP.2017.2670328, IEEE Transactions on Antennas and Propagation

β. The basic idea to estimate the electric field for an arbitrary β is to calculate these factors (a_1 and a_2) from few measured electric field data. As shown in Fig. 1, at a given point (or more generally, a plane or a volume), the electric fields for several relative phase combinations will be measured, and then the electric field for any other relative phase combination can be estimated from the measured data.

1) Expression for vector estimation: When the vector probes are used to measure the electric field, the proposed estimation is called vector estimation. The factors a_1 and a_2 in Eq. (3) can be determined within only measurements for different β values. To make it simple, the relative phases can be chosen as β = 0 and 180 degree. Then, the factors a_1 and a_2 can be calculated as

$$\begin{cases} a_1 &= (E_0 + E_{180})/2 \\ a_2 &= (E_0 - E_{180})/2, \end{cases} \tag{4}$$

where E_0 and E_{180} can be obtained directly from the electric field measurement using the vector probes for the relative phases of 0 and 180 degree, respectively.

Once a_1 and a_2 are determined, the electric field, thus the SAR, for an arbitrary β_{est} will be easily estimated by substituting the factors a_1 and a_2 from Eq. (4) into Eq. (3).

2) Expression for scalar estimation: Since the vector probes might be expensive, and not readily available, it is more useful to extend the estimation with the scalar probes. The estimation for the scalar electric field probes is referred to as scalar estimation.

Let $a_{1\mathrm{R}}$, $a_{2\mathrm{R}}$, $a_{1\mathrm{I}}$, and $a_{2\mathrm{I}}$ be the real and imaginary parts of a_1 and a_2, respectively. From Eq. (3), the square of the magnitude of the electric field, which is proportional to the SAR, can be expressed as

$$|E|^2 = b_1 + b_2 \cos\beta + b_3 \sin\beta \tag{5}$$

where

$$\begin{aligned} b_1 &= \left(a_{1\mathrm{R}}^2 + a_{1\mathrm{I}}^2\right) + \left(a_{2\mathrm{R}}^2 + a_{2\mathrm{I}}^2\right) \\ b_2 &= 2\left(a_{1\mathrm{R}} a_{2\mathrm{R}} + a_{1\mathrm{I}} a_{2\mathrm{I}}\right) \\ b_3 &= 2\left(a_{1\mathrm{I}} a_{2\mathrm{R}} - a_{1\mathrm{R}} a_{2\mathrm{I}}\right). \end{aligned} \tag{6}$$

By incorporating with σ and ρ from Eq. (1), we can obtain the formula of the SAR as

$$\mathrm{SAR} = c_1 + c_2 \cos\beta + c_3 \sin\beta, \tag{7}$$

where $c_i = b_i \sigma/\rho$ ($i = 1 \ldots 3$).

Now, in order to estimate the SARs for an arbitrary β_{est} from Eq. (7), we need to measure the SARs for three different relative phases. To make it simple, the relative phases can be chosen as β = 0, 90, and 180 degree. Then, the factors c_1, c_2, and c_3 can be derived from

$$\begin{aligned} c_1 &= \left(\mathrm{SAR}_0 + \mathrm{SAR}_{180}\right)/2, and \\ c_2 &= \left(\mathrm{SAR}_0 - \mathrm{SAR}_{180}\right)/2, and \\ c_3 &= \left(2\mathrm{SAR}_{90} - \mathrm{SAR}_0 - \mathrm{SAR}_{180}\right)/2, \end{aligned} \tag{8}$$

where SAR_0, SAR_{90}, and SAR_{180} are the SAR values for the relative phases of 0, 90, and 180 degree, respectively. They can be obtained directly from the SAR measurement using the scalar probes. The determined factors c_1, c_2, and c_3 are substituted into Eq. (7) to estimate the SARs for arbitrary values of β.

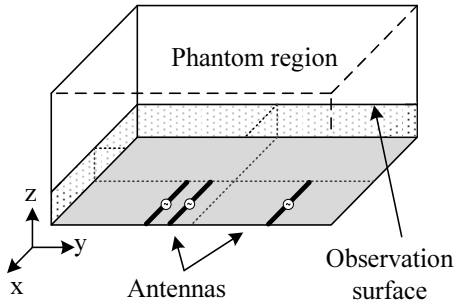

Fig. 2. N-antenna array and a phantom in SAR evaluation.

B. N-element antenna array

Figure 2 shows an example of the array that consists of *N* individual sources (antennas). Let us assume that each antenna is excited with each phase $\beta_i (i = 1..N)$. Without loss of generality, we can take $\beta_1 = 0$ (i.e., the first antenna is considered as a reference), and the other β_i is considered as the relative phase between the i^{th} antenna and the first antenna. The total electric field radiated by the *N* antennas is equal to the vector summation of all the individuals. To avoid duplication in electric field notations, the electric field at an evaluation point can be expressed as

$$E = a_1 e^{j\beta_1} + a_2 e^{j\beta_2} + \cdots + a_N e^{j\beta_N} \tag{9}$$

Again, note that the complex factors $\{a_1, a_2 \ldots a_N\}$ are independent of $\{\beta_1, \beta_2 \ldots \beta_N\}$. Thus, if we can calculate them from particular combinations of β, we will be able to estimate the electric fields with any arbitrary combinations of β. Similar to the two-antenna case, there will be two estimation methods that correspond to the types of electric field probes used in the SAR measurements.

1) Expression for vector estimation: The first stage of the vector estimation is to calculate the factors $\{a_1, a_2 \ldots a_N\}$ from measured data for pre-known relative phase combinations. We need to build up *N* equations to be able to determine $\{a_1, a_2 \ldots a_N\}$. Each equation corresponds to a measurement for a particular relative phase combination. Thus, the *N* equations can be expressed via *N* measurement times as

$$\begin{cases} E_1 &= a_1 e^{j\beta_{11}} + a_2 e^{j\beta_{12}} + \cdots + a_N e^{j\beta_{1N}} \\ E_2 &= a_1 e^{j\beta_{21}} + a_2 e^{j\beta_{22}} + \cdots + a_N e^{j\beta_{2N}} \\ \vdots & \\ E_N &= a_1 e^{j\beta_{N1}} + a_2 e^{j\beta_{N2}} + \cdots + a_N e^{j\beta_{NN}}, \end{cases} \tag{10}$$

which can be written as

$$\begin{bmatrix} E_1 \\ \vdots \\ E_N \end{bmatrix} = \begin{bmatrix} e^{j\beta_{11}} & \cdots & e^{j\beta_{1N}} \\ \vdots & \ddots & \vdots \\ e^{j\beta_{N1}} & \cdots & e^{j\beta_{NN}} \end{bmatrix} \begin{bmatrix} a_1 \\ \vdots \\ a_N \end{bmatrix}, \tag{11}$$

where $E_i\{i = 1 \ldots N\}$ is the measured electric field in the i^{th} measurement time, and β_{ij} $\{i = 1 \ldots N\}$; $\{j = 1 \ldots N\}$ is the relative phase β_j in the i^{th} measurement time.

The above equations can be solved as

This article has been accepted for publication in a future issue of this journal, but has not been fully edited. Content may change prior to final publication. Citation information: DOI 10.1109/TAP.2017.2670328, IEEE Transactions on Antennas and Propagation

$$\begin{bmatrix} a_1 \\ \vdots \\ a_N \end{bmatrix} = \begin{bmatrix} e^{j\beta_{11}} & \dots & e^{j\beta_{1N}} \\ \vdots & \ddots & \vdots \\ e^{j\beta_{N1}} & \dots & e^{j\beta_{NN}} \end{bmatrix}^{-1} \begin{bmatrix} E_1 \\ \vdots \\ E_N \end{bmatrix}. \quad (12)$$

The electric field for any arbitrary combinations of β_{est} can be easily estimated by substituting the factors $\{a_1, a_2 \dots a_N\}$ into Eq. (9). The required number of measurements for the vector estimation is exactly equal to the number of antennas (N). Thus, by using the vector electric field probe, this estimation method would significantly reduce the total SAR measurement time.

2) Expression for scalar estimation: Since the output of scalar electric field probes is proportional to the square of the magnitude of the measured electric field, it is useful to calculate the formula of the square of the magnitude of the electric field. From Eq. (9), it can be expressed as (see appendix for detailed calculations)

$$\begin{aligned} |E|^2 = &\left(\sum_{p=1}^{N}\left(a_{p\mathrm{R}}^2+a_{p\mathrm{I}}^2\right)\right) + \\ &+2\sum_{p=1}^{N-1}\sum_{q=2;q>p}^{N}\left(a_{p\mathrm{R}}a_{q\mathrm{R}}+a_{p\mathrm{I}}a_{q\mathrm{I}}\right)\cos\left(\beta_p-\beta_q\right) \\ &+2\sum_{p=1}^{N-1}\sum_{q=2;q>p}^{N}\left(a_{p\mathrm{R}}a_{q\mathrm{I}}-a_{p\mathrm{I}}a_{q\mathrm{R}}\right)\sin\left(\beta_p-\beta_q\right) \end{aligned} \quad (13)$$

where $a_{p\mathrm{R}}$ and $a_{p\mathrm{I}}$ are the real and imaginary parts of a_p.

Now, by incorporating σ and ρ in Eq. (1), the SAR of an N transmitting antenna device can be expressed in terms of the relative phases of the antennas as

$$\begin{aligned} \mathrm{SAR} = A &+ \sum_{p=1}^{N-1}\sum_{q=2;q>p}^{N} B_{pq}\cos\left(\beta_p-\beta_q\right) \\ &+ \sum_{p=1}^{N-1}\sum_{q=2;q>p}^{N} C_{pq}\sin\left(\beta_p-\beta_q\right) \end{aligned} \quad (14)$$

where A, B_{pq}, and C_{pq} are the real factors that can be expressed in terms of $a_{p\mathrm{R}}$, $a_{p\mathrm{I}}$, σ, and ρ.

Table I lists the SAR formulas for several numbers of antennas as examples (note that $\beta_1 = 0$) of the estimation using the scalar electric field probes. The SAR expression in Eq. (14) can be considered as a function of the relative phases of the sources. The function consists of $N(N-1)+1$ factors that do not depend on the change in the relative phases. Thus, the key technique to estimate the electric field with any arbitrary relative phase combinations is to determine these factors on the basic of the electric field data measured from several relative phase combinations. Because there are $N(N-1)+1$ factors, the required number of measurements would be $N(N-1)+1$.

The estimation methods for both the scalar and vector probes can be used to evaluate any arbitrary combination of the excitation phases of the sources (the antennas) in a multiple-antenna transmitting system. Because the required number of measurements is reduced, particularly for the vector estimation case, the total evaluation time would be significantly reduced.

C. Measurement procedure

The proposed estimation method plays an important role in measurement procedures to identify the relative phase combination that corresponds to the maximum SAR of the devices. At the initial step of the measurement, the input power to each antenna is set to its maximum in a normal communication as the maximum SAR usually corresponds to the maximum antenna input power. The next step is to measure the electric field/SAR on the area scan. The number of measurements depends on the SAR measurement systems with different types of electric field probe. After the area scan is completed for all the necessary measured data (different sets of relative phases), the estimation factors will be calculated according to Eq. (4) or (8) depending on the type of electric field probe. Once the estimation factors are determined, the SAR estimation can be computed with a phase step, 1 degree, for example. Using these factors, we can identify the relative phase combination β_{max} that corresponds to the maximum SAR. Thus, the next step is to set the relative phase as β_{max} and conduct the SAR measurement as a conventional procedure in area scan and zoom scan, and calculate the maximum spatial average SAR for 1g or 10g. The area and zoom scans are well defined in the SAR measurement standards [2], [3]. Obviously, to be able to set the relative phases of the sources, a test mode of the device under test should be provided by the manufacturers.

The proposed measurement procedure above clearly reduces the number of necessary measurements up to 2 or 3 measurements, depending on the type of electric field probes, for a two-antenna transmitting device. It can find the maximum value of the SAR and its related relative phase. The steps for the determination of the estimation factors can be performed by a computer thus, the total evaluation time will be significantly saved. Furthermore, the proposed procedure can work with the current SAR measurement systems that mainly employ scalar electric field probes. These advantages highlight the effectiveness of the proposed estimation method, thus, making it promisingly applicable. A similar procedure can be developed for the case of an N-antenna transmitting device. However, to make this paper concise, we only present here the measurement procedure for the two-antenna transmitting device.

TABLE I
EXPRESSIONS FOR SAR OF N-ANTENNA TRANSMITTERS

N	Number of measurements	Formula of SAR
2	3	$A + B\cos\beta + C\sin\beta$
3	7	$A + B_{12}\cos\beta_2 + B_{13}\cos\beta_3 + B_{23}\cos(\beta_2-\beta_3)$ $+C_{12}\sin\beta_2 + C_{13}\sin\beta_3 + C_{23}\sin(\beta_2-\beta_3)$
4	13	$A + B_{12}\cos\beta_2 + B_{13}\cos\beta_3 + B_{14}\cos\beta_4$ $+B_{23}\cos(\beta_2-\beta_3) + B_{24}\cos(\beta_2-\beta_4)$ $+B_{34}\cos(\beta_3-\beta_4) + C_{12}\sin\beta_2 + C_{13}\sin\beta_3$ $+C_{14}\sin\beta_4 + C_{23}\sin(\beta_2-\beta_3)$ $+C_{24}\sin(\beta_2-\beta_4) + C_{34}\sin(\beta_3-\beta_4)$

This article has been accepted for publication in a future issue of this journal, but has not been fully edited. Content may change prior to final publication. Citation information: DOI 10.1109/TAP.2017.2670328, IEEE Transactions on Antennas and Propagation

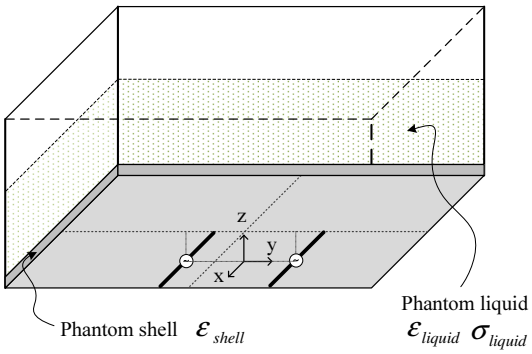

Fig. 3. Flat phantom used in numerical validations.

III. Numerical validations

A. Model 1

In order to demonstrate the validity of the proposed estimation method, finite-difference time-domain (FDTD) simulation results are used as measurement references. Simulation was carried out using the SEMCAD X software (SPEAG Switzerland) [12]. A flat phantom, shown in Fig. 3, is modeled in the simulation program. The geometrical parameters of the phantom as well as the antenna array are listed in Table II. Note that because the three components x, y, and z of electric fields can be explained for estimation in the same way, the estimation method will not depend on the field polarizations. Therefore, any antenna configurations with any polarization can be used for validations. To make it simple, the models in this section will be with one polarization.

The first model is a simple case with two dipole antennas working at 2450 MHz. The two dipoles are placed with a space of half wavelength (55 mm). We used the SAR values calculated from SEMCAD X instead of the measured ones. The SAR values, for the different relative phases (β) of 0, 90, and 180 degree, were calculated for the scalar estimation, whereas the SAR values, for β of 0 and 180 degree, were calculated for the vector estimation. After the estimation factors were determined using Eq. (4) or (8), we performed both the scalar and vector estimations for different relative phases, from 0 to 360 degree, with a phase step of 1 degree. The estimated and originally calculated SARs are normalized to the maximum value over the observation plane of the calculated SAR corresponding to β of 180 degree.

TABLE II
Parameters of the phantom and head tissue-equivalent liquid

Parameter			Value
Phantom size			180 × 180 × 150 mm^3
Shell thickness			2 mm
Liquid	Relative permittivity	@2.45 GHz	39.2
		@2.14 GHz	39.7
	Conductivity	@2.45 GHz	1.80 S/m
		@2.14 GHz	1.53 S/m
Shell	Relative permittivity	@2.45 GHz	3.7
		@2.14 GHz	3.7

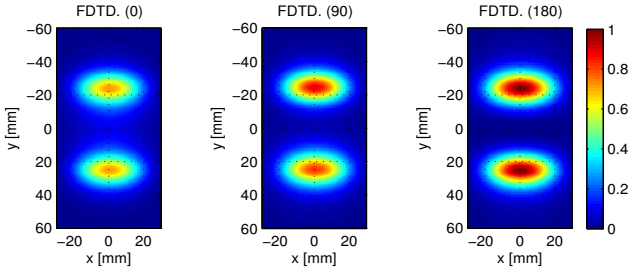

Fig. 4. SAR in a plane for β of 0, 90, and 180 degree.

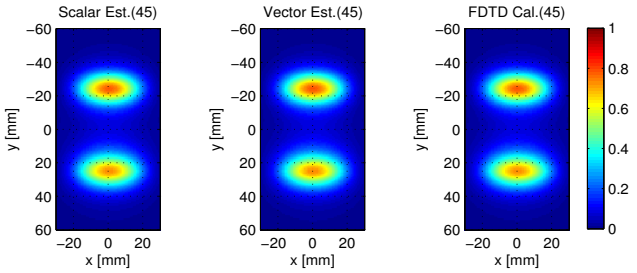

Fig. 5. A comparison between scalar-estimated, vector-estimated, and FDTD-simulated SAR for β of 45 degree.

Figure 4 shows the originally calculated SAR distributions in a plane for β of 0, 90, and 180 degree. As can be seen from this figure, the different relative phases result in the different SAR distributions. The estimation factors can be determined for the vector estimation according to Eq. (4) and for the scalar estimation according to Eq. (8). Then, the SARs for the arbitrary value of relative phases can be estimated using the estimation factors. Figure 5 shows a comparison between the scalar-estimated, vector-estimated, and FDTD-simulated SAR for β of 45 degree. Very good agreements between them can be found, and the difference at the maximum point SAR is only 0.06% for the scalar estimation and 0.37% for the vector estimation. This verifies that the proposed estimations work very well for both the vector or the scalar probes.

B. Model 2

The second model comes with more practical antennas. We take a model with two inverted F antennas (IFA) placed in a small case, similar to a mobile phone. The antennas work at 2140 MHz. The antenna configuration, its dimensions, and the phantom in the simulation are shown in Fig. 6. Again, the calculated SAR for β of 0, 90, and 180 degree, were used for the scalar estimation and those for β of 0 and 180 degree were used for the vector estimation to calculate estimation factors.

Figure 7 illustrates the SAR distributions for the three pre-known relative phases, i.e., β of 90 and 180 degree. We can see that owing to the vector summation of the electric fields from individual antennas, the SAR peak point on the observation plane may not be at the location of each antenna. We also found good agreements between both the vector and scalar estimations and the original FDTD calculation in Fig. 8 for the relative phase of 45 degree. The differences between them in this case are 0.005% and 0.034% for the scalar and vector

This article has been accepted for publication in a future issue of this journal, but has not been fully edited. Content may change prior to final publication. Citation information: DOI 10.1109/TAP.2017.2670328, IEEE Transactions on Antennas and Propagation

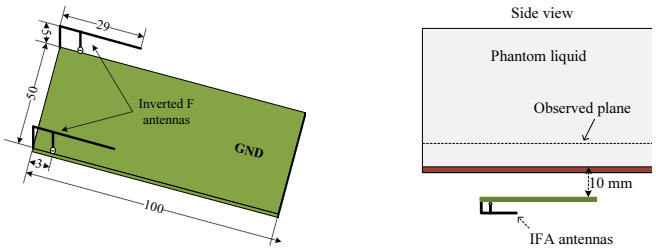

(a) (b)

Fig. 6. IFA models: (a) Antennas; (b) Phantom in simulation. All dimension in [mm].

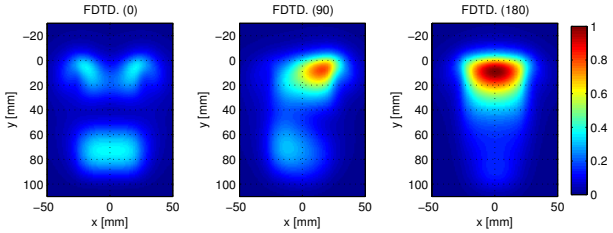

Fig. 7. SAR distributions of the three pre-known relative phases: 0, 90, an 180 degree.

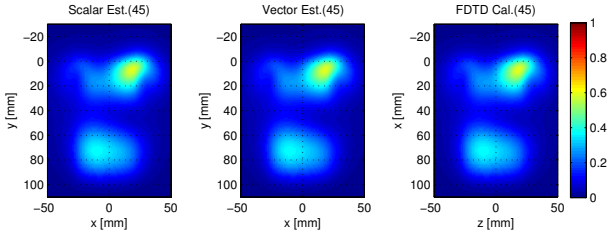

Fig. 8. Comparisons between the scalar-estimated, vector-estimated, and originally FDTD-simulated SAR for β of 45 degree.

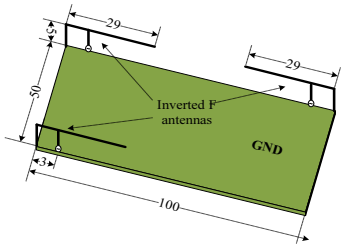

Fig. 9. IFA in model 3. All dimensions in [mm].

estimations, respectively. These minor differences verify the validity of the proposed estimation method.

C. Model 3

In the third model, we extend the validations with a three-antenna option. Three IFAs allocated in a small case similar to the second model are developed. The antenna configuration and dimensions are shown in Fig. 9, and the setup of the antennas and phantom is similar to that shown in Fig. 6(b) in the second model.

In the three-antenna case, the vector estimation requires the measurements of electric fields for 3 different relative phase combinations, and the scalar estimation requires the

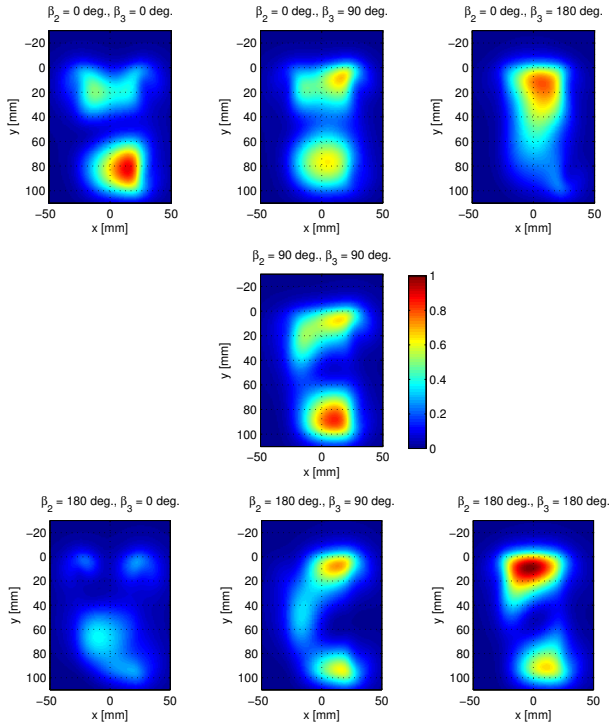

Fig. 10. SAR distributions of 7 pre-known relative phases for estimation of the case of 3 antennas.

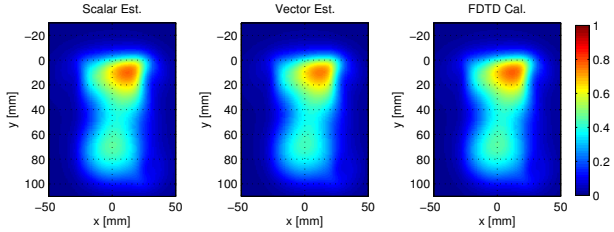

Fig. 11. Comparisons between calculated SAR and estimated SAR for β_2 = 0 degree, β_3 = 135 degree for the three-antenna case.

measurements of electric fields for 7 different relative phase combinations. To make it simple in the following estimations, the 3 relative phase combinations for the vector estimation are chosen as

- Pattern 1 for β_2 = 0 degree, β_3 = 0 degree,
- Pattern 2 for β_2 = 0 degree, β_3 = 180 degree, and
- Pattern 3 for β_2 = 180 degree, β_3 = 180 degree.

For the scalar estimation, 7 necessary measurements will be conducted for different relative phase combinations, as follows:

- Pattern 1 for β_2 = 0 degree, β_3 = 0 degree,
- Pattern 2 for β_2 = 0 degree, β_3 = 90 degree,
- Pattern 3 for β_2 = 0 degree, β_3 = 180 degree,
- Pattern 4 for β_2 = 90 degree, β_3 = 90 degree,
- Pattern 5 for β_2 = 180 degree, β_3 = 0 degree,
- Pattern 6 for β_2 = 180 degree, β_3 = 90 degree, and
- Pattern 7 for β_2 = 180 degree, β_3 = 180 degree.

All calculated and estimated SARs for this model are normalized to the maximum calculated SAR obtained from the pattern for β_2 = 180 degree, and β_3 = 180 degree. Figure

This article has been accepted for publication in a future issue of this journal, but has not been fully edited. Content may change prior to final publication. Citation information: DOI 10.1109/TAP.2017.2670328, IEEE Transactions on Antennas and Propagation

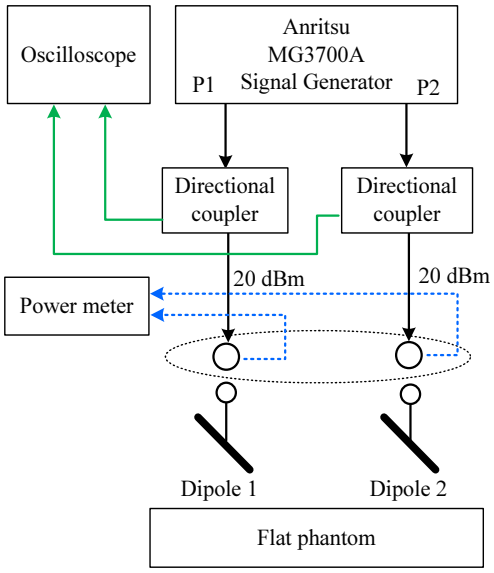

Fig. 12. Experimental scheme.

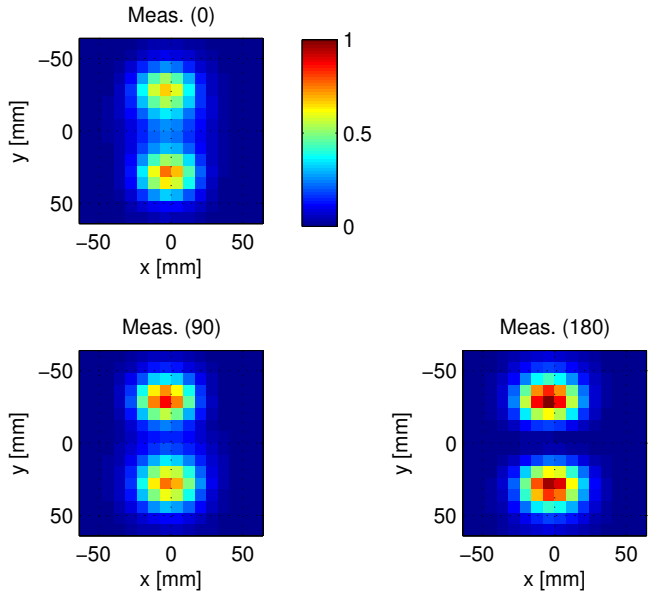

Fig. 13. Normalized measured SAR for β of 0, 90, and 180 degree.

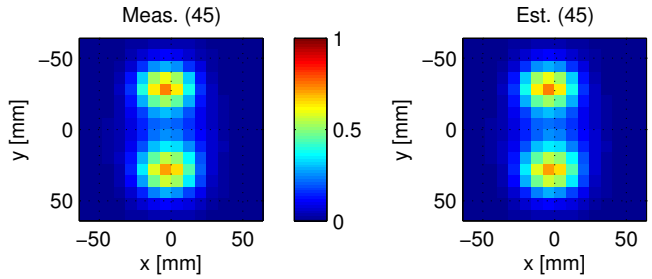

Fig. 14. Comparisons between measured and scalar-estimated SAR for β of 45 degree.

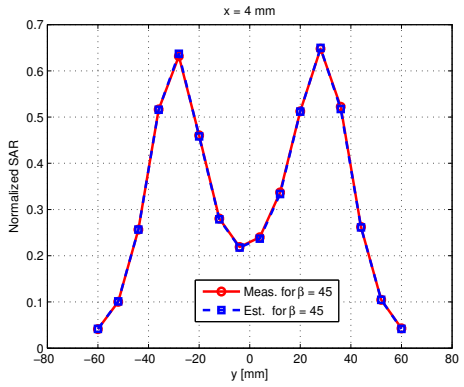

Fig. 15. Measured and scalar-estimated SAR for β of 45 degree.

10 shows the SAR distributions for the seven relative phase combinations, which include the three necessary combinations for the vector estimation. Again, we can see that the different relative phase combinations result in the different SAR distributions and SAR values. On the basic of these data, the SARs for other relative phase combinations can be estimated according to Eqs. (9) and (14) for $N = 3$. Figure 11 shows a comparison between FDTD-calculated and estimated SAR distributions for $\beta_2 = 0$ degree and $\beta_3 = 135$ degree. As can be seen from this figure, the calculated SARs agree well with both the vector-estimated and the scalar-estimated SARs. The difference between them at the maximum SAR point is about 1% for the scalar estimation and 2% for the vector estimation.

In general, different cases with different antenna types, antenna configurations, antenna numbers, and so on can also be applicable with the estimation methods. Thus far, we have achieved very good agreements between the calculated and estimated SARs for all of the examined cases.

IV. Experimental Validations

A. Experimental configuration

In order to verify the proposed method, several SAR measurements using the DASY52 systems [13] have been carried out. Since the DASY52 system in our laboratory works with a scalar electric field probe, we will only be able to validate the scalar estimation. Figure 12 illustrates the experimental scheme of our measurements. The flat phantom (ELI4) and two co-polarized dipoles, operated at 2.45 GHz and with the spacing of 0.5λ, are used in our experiments. The distance between the dipoles and the phantom is 10 mm. Continuous wave (CW) signals, generated from a two-port signal generator (Anritsu Vector Signal Generator MG3710A), are connected to the antennas via two identical RF directional couplers and coaxial cables. The relative phase of the two signals, β, can be controlled by setting in the signal generator, and can be checked by using an oscilloscope (Agilent Infiniun DSA90804A). The output powers in our experiments for two antennas are equal to 20 dBm.

The SARs on the 2D plane at z = 4 mm were measured for the proposed estimations (the inner surface of the phantom is at z = 0 mm). Along each of the x- and y-axes, there were 16 measured points spacing 8 mm linearly. In total, 256 points were measured at the observation plane. The size of the plane, therefore, is 120 $\times$ 120 mm^2. The measurement system will repetitively measure the SARs at these points for

This article has been accepted for publication in a future issue of this journal, but has not been fully edited. Content may change prior to final publication. Citation information: DOI 10.1109/TAP.2017.2670328, IEEE Transactions on Antennas and Propagation

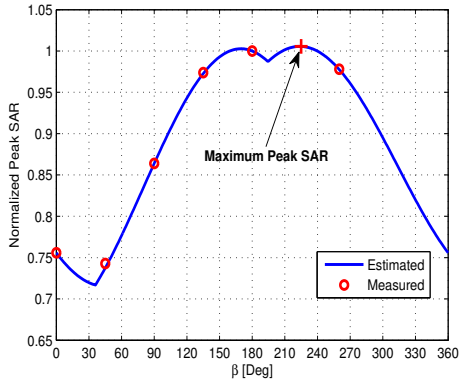

Fig. 16. Normalized peak estimated SAR for β = [0...360 degree].

different β values. Note that the SAR values were obtained for the proposed estimations, i.e., all three components of the electric field (i.e. E_x, E_y, and E_z) are taken into account.

B. Measured and estimated results

Six measurements, corresponding to the relative phase β of $0, 45, 90, 135, 180$, and 260 degree, have been carried out. Among them, the SAR values corresponding to β of $0, 90$, and 180 degree are used to determine the estimation factors illustrated in Eq. (8). The others will be used to compare with the estimated SAR for the same relative phase β. All of the measured and estimated SARs have been normalized with the maximum value of SAR for β of 180 degree.

Figure 13 shows the normalized measured SAR for β of $0, 90$, and 180 degree in the observation plane. As can be seen from the figure, the SAR distribution changes for the different β values. Figures 14 and 15 show the comparisons between the measured and estimated SARs for the relative phase of 45 degree. The normalized 2D SARs at the observation plane are shown in Fig. 14 and the normalized 1D SARs where x = 4 mm are shown in Fig. 15. As can be seen from these figures, the estimated SARs agree very well with the measured ones.

By applying the proposed estimation method, we can find the β value corresponding to the maximum SAR. Fig. 16 shows the normalized peak SAR when β changes in the range of [0 ... 360 degree] with steps of 1 degree. In total, 360 estimations have been performed in a short time to obtain this figure. Indeed, measuring SAR for such numbers of the relative phases would be impractical, given that each measurement typically takes about 30 min. As can be seen from this figure, the maximum peak SAR corresponds to the relative phase β of 225 degree. Moreover, we can also see the good agreements between the measured and the estimated maximum SARs for β of $45, 135$, and 260 degree.

C. Deviation evaluation

In order to highlight the validity of the estimation methods, it would be useful to calculate the error of the estimation. Let $\overline{\mathrm{SAR}}_{meas}$ and $\overline{\mathrm{SAR}}_{est}$ be the normalized SARs at the observation plane, obtained from the measurement and the estimation, respectively. $\overline{\mathrm{SAR}}$ indicates the normalized SAR. The deviation

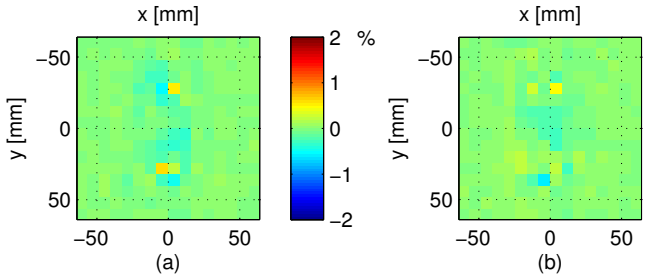

Fig. 17. Deviation calculated for different values of β: (a) β of 45 degree, (b) β of 135 degree.

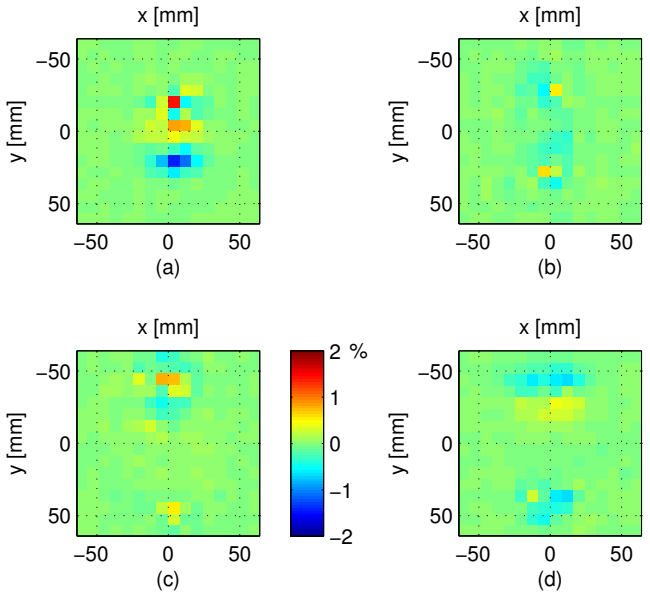

Fig. 18. Deviation calculated for β = 45 degree for different measured cases: (a) 2450 MHz, spacing 0.25λ, (b) 2450 MHz, spacing 0.5λ, (c) 2450 MHz, spacing 1λ, and (d) 2140 MHz, spacing 0.5λ.

of estimation is defined as the difference between the two normalized values and can be written as

$$Dev = 100 \cdot (\overline{\mathrm{SAR}}_{est} - \overline{\mathrm{SAR}}_{meas}) \quad [\%]. \tag{15}$$

Figure 17 shows the deviations calculated for β of 45 and 135 degree according to Eq. (15). The color bar, indicated as the deviation, shows the difference in percentage. We can see that the differences between the measured and the estimated SARs are within 2% for all the examined values of β. These confirm that the estimation works well with the measured data obtained from the actual SAR measurement. Thus, the proposed estimation method is very promisingly applicable in the SAR evaluation for multiple-antenna transmitting devices.

D. Other validations

In order to extend the investigation on the performance of the proposed estimation methods, we have carried out several SAR measurements for other types of antenna array including changing antenna configurations, the distance between antennas, and operating frequency. The experimental scheme and observation plane are kept the same as mentioned in the previous section. Again, the measured SARs for β of $0, 90$,

This article has been accepted for publication in a future issue of this journal, but has not been fully edited. Content may change prior to final publication. Citation information: DOI 10.1109/TAP.2017.2670328, IEEE Transactions on Antennas and Propagation

and 180 degree are used for determining the factors for the estimation, and the measured SARs for β of 45 degree are obtained as references to compare with the estimated SARs for the same value of β. As a result, good agreement between the measured and estimated SARs can be achieved, regardless of the antenna configurations, distance between antennas, or different frequencies. Figure 18 shows the deviation calculated according to Eq. (15) for different examined cases, including two antennas working at 2450 and 2140 MHz. The distance between them varies in different configurations such as 0.25λ, 0.5λ, and 1λ. Here, we can see that although there is a strong mutual coupling where the antennas are spaced a quarter of wavelength (0.25λ), the deviation between estimated and measured SARs is kept below 2%. For weaker mutual couplings between the antennas with a spacing of 1λ or 0.5λ, the deviations are still below 2%. Furthermore, the deviation between the estimated and measured SARs for different operating frequencies (2450 MHz vs. 2140 MHz) is also small, as shown in Fig. 18(d). These deviations validate the accuracy of the proposed method regardless of the mutual couplings between the transmitting antennas and their operating frequencies.

V. Comparisons with conventional techniques

Reducing the number of necessary measurements and being able to identify the maximum SAR using the measurements with the limited different relative phase combinations are the notable advantages of the proposed estimation method. Compared with the conventional measurement technique [2], [3], [9], which requires the measurement of every relative phase combination, the proposed method significantly reduces time and effort in the SAR evaluation.

Table III lists a comparison between the two techniques. For example, if the phase step in the conventional method is equal to 1 degree, there will be 360 repetitive measurements in order to find the maximum SAR of a two-element antenna transmitter, given that each measurement typically takes about 30 min. Instead, the proposed method only requires 3 measurements, i.e., reducing 99.17% (357/360) the measurement time.

Furthermore, when the number of antennas is increased, the conventional technique soon becomes impractical while the proposed technique is still manageable. When N=3, while the proposed technique only requires 7 measurements, the conventional technique requires 129600 measurements for the phase step of 1 degree. Clearly, the proposed technique outperforms the conventional one, and will be a promising method for compliance tests.

In addition, because the proposed method can be applicable for the systems utilizing vector probes, or more particularly, vector probe arrays such as the one in ref. [14], applying it to those systems can lead to a very short measurement time.

TABLE III
Comparison between a conventional technique in IEC-TR 62630/IEEE-1528 standards and the proposed technique for SAR measurement systems utilizing scalar electric probes

		Conventional technique [2] [3]		Proposed technique
Two ant.	Number of meas.	360	36	**3**
	Time [h]	180	18	1.5
	Resolution	if phase step is 1 degree	if phase step is 10 degree	Arbitrary phase step
Three ant.	Number of meas.	129600	1296	**7**
	Time [h]	64800	648	3.5
	Resolution	if phase step is 1 degree	if phase step is 10 degree	Arbitrary phase step
Four ant.	Number of meas.	46656000	46656	**13**
	Time [h]	23328000	23328	6.5
	Resolution	if phase step is 1 degree	if phase step is 10 degree	Arbitrary phase step

VI. Conclusion

In this paper, we present the fast estimation methods for evaluating the specific absorption rate of multiple-antenna transmitting devices. The proposed method is based on the SARs at a given point for different relative phase combinations of the antennas. Theoretical analyses have been shown for both vector and scalar electric field probe uses. Generally, to evaluate the SAR of an N-antenna transmitting device, only N measurements are necessary if the vector electric field probe is used in a measurement system, whereas $N(N-1)+1$ measurements should be carried out if the measurement system utilizes the scalar electric field probes.

In addition, the validity of the proposed method has been confirmed by both numerical simulations and actual SAR measurements for various antenna configurations and operating frequencies. It indicates that the estimation works well in most examined cases, and the errors caused by the proposed estimation method are very small, mainly kept under a few percent of the maximum measured SAR.

Finally, thanks to a limited number of necessary measurements, the proposed technique significantly reduces the total evaluation time for a device in a compliance test, yet can still provide an accurately estimated SAR. It is believed that the proposed technique will soon be applied in compliance tests for multiple-antenna transmitting devices.

Acknowledgment

This research is supported by the Vietnam National Foundation for Science and Technology Development (NAFOSTED) under grant number 102.04-2014.16. It is also supported in part by the Ministry of Internal Affairs and Communications, Japan.

Appendix

Below is the proof of the SAR formula in Eq. (14). Equation. (14) can be written in terms of the real and the imaginary parts of a_p $\{p = 1, \ldots, N\}$ as

$$E = \sum_{p=1}^{N} (a_{p\mathrm{R}} + j a_{p\mathrm{I}})(\cos\beta_p + j \sin\beta_p) \qquad (16)$$

or

This article has been accepted for publication in a future issue of this journal, but has not been fully edited. Content may change prior to final publication. Citation information: DOI 10.1109/TAP.2017.2670328, IEEE Transactions on Antennas and Propagation

$$E = \left(\sum_{p=1}^{N} a_{p\mathrm{R}} \cos\beta_p - \sum_{p=1}^{N} a_{p\mathrm{I}} \sin\beta_p\right) + j\left(\sum_{p=1}^{N} a_{p\mathrm{I}} \cos\beta_p + \sum_{p=1}^{N} a_{p\mathrm{R}} \sin\beta_p\right) \tag{17}$$

The square of the magnitude of the measured electric field can be then expressed as

$$|E|^2 = \left(\sum_{p=1}^{N} a_{p\mathrm{R}}\cos\beta_p \ - \sum_{p=1}^{N} a_{p\mathrm{I}}\sin\beta_p \ \right)^2 + \left(\sum_{p=1}^{N} a_{p\mathrm{I}}\cos\beta_p \ + \sum_{p=1}^{N} a_{p\mathrm{R}}\sin\beta_p \ \right)^2 \tag{18}$$

which can be written as

$$\begin{aligned}|E|^2 = &\left(\sum_{p=1}^{N} a_{p\mathrm{R}}\cos\beta_p \ \right)^2 + \left(\sum_{p=1}^{N} a_{p\mathrm{I}}\sin\beta_p \ \right)^2 \\ &-2\sum_{p=1}^{N}\sum_{q=1}^{N} a_{p\mathrm{R}}\cos\beta_p \ a_{q\mathrm{I}}\sin\beta_q \\ &+\left(\sum_{p=1}^{N} a_{p\mathrm{I}}\cos\beta_p \ \right)^2 + \left(\sum_{p=1}^{N} a_{p\mathrm{R}}\sin\beta_p \ \right)^2 \\ &+2\sum_{p=1}^{N}\sum_{q=1}^{N} a_{p\mathrm{I}}\cos\beta_p \ a_{q\mathrm{R}}\sin\beta_q\end{aligned} \tag{19}$$

Expanding the right side of the above equation, we have

$$\begin{aligned}|E|^2 = &\sum_{p=1}^{N} a_{p\mathrm{R}}^2\cos^2\beta_p \ + 2\sum_{p=1}^{N-1}\sum_{q=2;q>p}^{N} a_{p\mathrm{R}}a_{q\mathrm{R}}\cos\beta_p \ \cos\beta_q \\ &+\sum_{p=1}^{N} a_{p\mathrm{I}}^2\sin^2\beta_p \ + 2\sum_{p=1}^{N-1}\sum_{q=2;q>p}^{N} a_{p\mathrm{I}}a_{q\mathrm{I}}\sin\beta_p \ \sin\beta_q \\ &-2\sum_{p=1}^{N-1}\sum_{q=2;q>p}^{N} a_{p\mathrm{R}}a_{q\mathrm{I}}\cos\beta_p \ \sin\beta_q \\ &-2\sum_{p=1}^{N-1}\sum_{q=2;q>p}^{N} a_{p\mathrm{I}}a_{q\mathrm{R}}\sin\beta_p \ \cos\beta_q \\ &+\sum_{p=1}^{N} a_{p\mathrm{I}}^2\cos^2\beta_p \ + 2\sum_{p=1}^{N-1}\sum_{q=2;q>p}^{N} a_{p\mathrm{I}}a_{q\mathrm{I}}\cos\beta_p \ \cos\beta_q \\ &+\sum_{p=1}^{N} a_{p\mathrm{R}}^2\sin^2\beta_p \ + 2\sum_{p=1}^{N-1}\sum_{q=2;q>p}^{N} a_{p\mathrm{R}}a_{q\mathrm{R}}\sin\beta_p \ \sin\beta_q \\ &+2\sum_{p=1}^{N-1}\sum_{q=2;q>p}^{N} a_{p\mathrm{R}}a_{q\mathrm{I}}\sin\beta_p \ \cos\beta_q \\ &+2\sum_{p=1}^{N-1}\sum_{q=2;q>p}^{N} a_{p\mathrm{I}}a_{q\mathrm{R}}\cos\beta_p \ \sin\beta_q\end{aligned} \tag{20}$$

Now, by grouping common terms in Eq. (20), we can obtain the final expression of Eq. (14).

$$\begin{aligned}|E|^2 = &\left(\sum_{p=1}^{N}\left(a_{p\mathrm{R}}^2+a_{p\mathrm{I}}^2\right)\right) + \\ &+2\sum_{p=1}^{N-1}\sum_{q=2;q>p}^{N}\left(a_{p\mathrm{R}}a_{q\mathrm{R}} + a_{p\mathrm{I}}a_{q\mathrm{I}}\right)\cos\left(\beta_p - \beta_q\right) \\ &+2\sum_{p=1}^{N-1}\sum_{q=2;q>p}^{N}\left(a_{p\mathrm{R}}a_{q\mathrm{I}} - a_{p\mathrm{I}}a_{q\mathrm{R}}\right)\sin\left(\beta_p - \beta_q\right)\end{aligned} \tag{21}$$

REFERENCES

[1] ICNIRP, "Guidelines for limiting exposure to time-varying electric, magnetic and electromagnetic fields (up to 300 GHz)," *Health Phys.*, vol. 74, pp. 494-522, 1998.

[2] IEC 62209-2, "Human exposure to radio frequency fields from hand-held and body-mounted wireless communication devices - Human models, instrumentation, and procedures Part 2: Procedure to determine the specific absorption rate (SAR) for wireless communication devices used in close proximity to the human body (frequency range of 30 MHz to 6 GHz)", Ed. 1.0, 2010.

[3] IEEE 1528, "IEEE Recommended Practice for Determining the Peak Spatial-Average Specific Absorption Rate (SAR) in the Human Head from Wireless Communications Devices: Measurement Techniques", Ed. 2013.

[4] M. Y. Kanda, M. G. Douglas, E. D. Mendivil, M. Ballen, A. V. Gessner, and C-K. Chou, Faster determination of mass-averaged SAR from 2-D area scans, IEEE Trans. Microw. Theory Tech., vol. 52, no. 8, 2004, pp. 2013-2020.

[5] M. Manning and P. Massey, "Rapid SAR testing of mobile phone prototype using a spherical test geometry," IEE Technical Seminar on Antenna Measurements and SAR (AMS 2002), Loughborough University, UK, May, 28-29 2002.

[6] B. Derat, O. Merckel, J-C. Bolomey, and G. Fleury, "Rapid parametric SAR reconstruction from a small number of measured E-field data: validation of an ellipsoidal model", European Cooperation in the Field of Scientific and Technical Research, COST 273 TD(03)098, 21-23 May, 2003, Paris, France.

[7] B. Thors, A. Thielens, J. Friden, D. Colombi, C. Tornevik, G. Vermeeren, L. Martens, W. Joseph, "Radio frequency electromagnetic field compliance assessment of multi-band and MIMO equipped radio base stations," Bioelectromagnetics, vol. 35, iss. 4, pp. 296-308, May 2014.

[8] E. Degirmenci, B. Thors, C. Tornevik, "Assessment of Compliance With RF EMF Exposure Limits: Approximate Methods for Radio Base Station Products Utilizing Array Antennas With Beam-Forming Capabilities," *IEEE Trans, on Electromag. Compat.*, vol. 58, iss. 4, pp. 1110 - 1117, Aug. 2016.

[9] IEC/TR 62630, "Guidance for Evaluating Exposure from Multiple Electromagnetic Sources", Ed. 1.0, 2010.

[10] T. Iyama and T. Onishi, "Maximum Average SAR Measurement Procedure for Multi-Antenna Transmitters", *IEICE Trans. Comm.*, vol. E93-B, no. 7, pp. 1821-1825, Jul. 2007.

[11] D. T. Le, T. Iyama, L. Hamada, S. Watanabe, and T. Onishi, "Averaging Time Required for Measuring the Specific Absorption Rate of a MIMO Transmitter" in *IEEE EMC Magazine*, Vol. 3, Quarter 1, pp 51-57, 2014.

[12] SEMCAD-X by SPEAG, http://www.speag.com/products/semcad/overview/

[13] DASY52 by SPEAG, http://www.speag.com/products/dasy/dasy-systems/

[14] ART-MAN by ART-Fi, http://www.art-fi.eu/art-man

This article has been accepted for publication in a future issue of this journal, but has not been fully edited. Content may change prior to final publication. Citation information: DOI 10.1109/TAP.2017.2670328, IEEE Transactions on Antennas and Propagation

Dinh Thanh Le (S'11M'14) received his Ph.D. degree from the University of Electro-Communications (UEC), Tokyo, Japan in 2012. From May 2012 to Aug. 2014, he was a researcher at the Electromagnetic Compatibility Laboratory, National Institute of Information and Communications Technology (NICT), Japan. Since Sep. 2014, he is a lecturer of Le Quy Don Technical University, Hanoi, Vietnam. His research expertise is in the area of applied electromagnetics, including the topics of bioelectromagnetics, SAR measurement techniques, and designs of broadband antennas. Le was the recipient of the Research Activities Award from the University of Electro-Communications, Tokyo, in 2012. He also received the Best Paper Award during the 2012 TriSAI conference, Young Scientist Excellent Paper Award during the 2012 Pan-Pacific EMC Joint Meeting (PPEMC'12) organized by EMCJ, Japan, and Student Paper Competition Honorable Mention during the IEEE 2011 AP-S Symposium and USNC/URSI Meeting held in Washington, US, and he was one of the finalists for Best Measurement Paper Award during the EuCAP 2015 conference.

Lira Hamada received her Ph.D. degree from Chiba University, Chiba, Japan, in 2000. From 2000 to 2005, she was with the Department of Electronics Engineering, The University of Electro-Communications, Tokyo, Japan. Since 2005, she has been with the National Institute of Information and Communications Technology, Tokyo. She is a researcher responsible for the measurement and calibration technique for the specific absorption rate evaluation system, including the standardization activity.

Soichi Watanabe (S'93M'96) received his B.E., M.E., and D.E. degrees in electrical engineering from Tokyo Metropolitan University, Tokyo, Japan, in 1991, 1993, and 1996, respectively. He is currently with the National Institute of Information and communications Technology (NICT), Tokyo, Japan. His research interests include biomedical electromagnetic compatibility. Dr. Watanabe is a member of the Institute of Electronics, Information, and Communication Engineers (IEICE), Japan, the Institute of Electrical Engineers, Japan, and the Bioelectromagnetics Society. Since 2004, he has been a member of the Standing Committee on Physics and Engineering of the International Commission on Non-Ionizing Radiation Protection. He was the recipient of several awards, including the 1996 International Scientist Radio Union Young Scientist Award and the 1997 IEICE Best Paper Award.

Teruo Onishi (M'01) received his B.S. degree in physics from the Tokyo University of Science, Tokyo, Japan, in 1987, and his D.E. degree from the Graduate School of Science and Technology, Chiba University, Chiba, Japan, in 2005. He was with Toyo Communication Equipment Company, Ltd., and Nippon Ericsson K.K. From 1990 to 1992, he worked on finite-difference time-domain (FDTD) analysis for solving electromagnetic problems at Hokkaido University, Sapporo, Japan. He is currently a Senior Research Engineer in the Radio Frequency Technology Research Group, Research Laboratories, NTT DOCOMO, Inc., Kanagawa, Japan. His current research interests include the standardization of SAR measurement and the study of electromagnetic field (EMF), the FDTD method, antennas for mobile terminals, and printed antennas. Dr. Onishi is a member of the Institute of Electronics, Information, and Communication Engineers (IEICE) and the Bioelectromagnetics Society (BEMS). He is also the Secretary of the Technical Group on Applications of Body Area Radiowaves of the IEICE. He is also a member of the International Electrotechnical Committee (IEC), Project Team 62209, and the IEEE Standards Coordinating Committee 34, Subcommittee 2.